Pramana – J. Phys., Vol. 38, No. 1, January 1992, pp. 77–90. © Printed in India.

Effect of distortion in electron impact excitation in Coulomb-projected Born approximation

V KUMAR, B N ROY and D K RAI*

Department of Physics, Bihar University, Muzaffarpur 842001, India
*Department of Physics, Banaras Hindu University, Varanasi 221005, India

MS received 31 January 1991; revised 18 July 1991

Abstract. We have calculated total and differential cross-sections for $1s \rightarrow ns$ $(n = 2, 3, 4)$ electron impact excitation of hydrogen and hydrogenic ions at various energies in Coulomb-projected Born approximation. Distortion due to static interactions, target polarization and exchange effects has been incorporated in the initial channel. The present calculations have been compared with other theoretical and experimental results.

Keywords. Coulomb-projected Born method; distorted wave; electron impact excitation; exchange potential; target polarization.

PACS No. 34·80

1. Introduction

Distorted-wave approximations are widely used in atomic scattering theory, partially due to interest in plasma where the presence of long range electrostatic interaction suggests a need to include Coulomb distortion. Among the theoretical approaches, there are two major sources of error in the evaluation of scattering amplitude. These are either in the choice of the approximate method adopted for calculation or in using the inaccurate input wave function. In the intermediate and high energy regions attempts have been made to improve the first Born approximation by taking into account the effect of the nuclear interaction term in the form of distorted waves (screened Coulomb waves). Geltman and Hidalgo (1971) introduced the Coulomb-projected Born approximation (CPBA) in which pure Coulomb waves are taken in the final channel only. Stauffer and Morgan (1975) generalized the CPBA by taking a free parameter δ to account for screening. Shaver and Stauffer (1980) modified the generalized CPBA by introducing a screening parameter which varies with distance between the incident particle and the target nucleus and calculated the elastic and inelastic cross-sections for electron-hydrogen collision.

The distorted wave model and its variants have proved to be successful in predicting the cross-sections at intermediate and high energies. McDowell *et al* (1973) have incorporated the distortion only in initial channel due to static interaction, target polarization and exchange effects and obtained satisfactory results. In the usual CPBA, plane waves are taken in the initial channel and Coulomb waves in the final channel. In order to obtain satisfactory results at intermediate and low energies it becomes essential to include distortion effects. When the electron is far from the atom it sees the residual charge on the atomic system, which is zero for neutral atoms. On the

other hand, when the incident electron is close to the nucleus, the electron sees the full charge of the nucleus without electron screening. So it is desirable to take into account short-range static interaction term induced distortion in the initial channel.

In view of the above mentioned facts, we have incorporated distortions due to static interaction, target polarization and exchange effects in the initial channel along the line suggested by McDowell *et al* (1973) in the Coulomb-projected Born (CPB) method. With this modification we expect to get better results than those obtained by using the CPB method, because the plane wave in the initial channel is now replaced by a distorted wave (which is closer to the actual physical situation of the process) for the projectile electron. We also expect these results to be better than the distorted-wave polarized orbital (DWPO) method of McDowell *et al* (1973) as the effect of incident electron nucleus interaction is included in T-matrix in the form of the Coulomb waves χ_{kq} in the final channel. This work is connected with the DWPO model of McDowell *et al* (1973) in the same way as the CPBA with the plane wave Born approximation. The purpose is to see how the inclusion of distortion in the initial channel affects the results of the CPB method.

2. Theory

CPB approximation was formulated by Geltman (1971), making use of the fact that one may split the total Hamiltonian H of the system arbitrarily into an unperturbed part H_0 and a perturbation V. The most common choice is to assume that the unperturbed part consists of a non-interacting incident electron and the target atom. The theory developed below is for a hydrogen atom and an incident electron

$$H_0 = -\frac{1}{2}\nabla_1^2 - \frac{1}{2}\nabla_2^2 - \frac{Z}{r_1}, \tag{1}$$

$$V = -\frac{Z}{r_2} + \frac{1}{r_{12}}, \tag{2}$$

$\mathbf{r}_1$ and $\mathbf{r}_2$ represent the coordinates of the target electron and projectile electron, respectively.

The T-matrix for the transition from initial state p to final state q may be written as

$$T_{pq} = \left\langle e^{i\mathbf{k}_q\cdot\mathbf{r}_2}\phi_q(\mathbf{r}_1)\left| -\frac{Z}{r_2} + \frac{1}{r_{12}}\right|\psi_p^+(\mathbf{r}_1,\mathbf{r}_2)\right\rangle. \tag{3}$$

ϕ_q is the final state of the atom, $\mathbf{k}_q$ is the final wave-vector of the projectile and ψ_p^+ is the total exact scattering wave function.

Geltman (1971) included the projectile electron and target nucleus interaction term in the unperturbed part of the Hamiltonian and thus

$$H_0 = -\frac{1}{2}\nabla_1^2 - \frac{1}{2}\nabla_2^2 - \frac{Z}{r_1} - \frac{Z}{r_2}. \tag{4}$$

$$V = \frac{1}{r_{12}}. \tag{5}$$

The corresponding T-matrix takes the form

$$T_{pq} = \left\langle \chi_{k_q}(Z, \mathbf{r}_2)\phi_q(\mathbf{r}_1)\left|\frac{1}{r_{12}}\right|\psi_p^+(\mathbf{r}_1, \mathbf{r}_2)\right\rangle. \tag{6}$$

The usual Born approximation and the CPBA are obtained by replacing the exact scattering solution ψ_p^+ by $\exp(i\mathbf{k}_p\cdot\mathbf{r}_2)\phi_p(\mathbf{r}_1)$ in (3) and (6), respectively. ϕ_p is the wave-function of the target atom in the initial state. The CPB method has been found to be better than Born approximation for electron-atom collision process.

In order to improve upon the CPB method we replace ψ_p^+ by $\mathscr{A}F^{\pm}(\mathbf{r}_2)\phi_p(\mathbf{r}_1)$ where $F^{\pm}(\mathbf{r}_2)$ is the distorted wave and $\mathscr{A}$ is the antisymmetrization operator. The distorted wave is derived by the procedure adopted by McDowell *et al* (1973). Thus, $F^{\pm}(\mathbf{r}_2)$ is expanded in partial waves

$$F^{\pm}(\mathbf{r}_2) = k_p^{-1/2} r_2^{-1} \sum_{l=0}^{\infty} (2l+1) i^l \exp(i\delta_l^{\pm}) U_l(k_p, r_2) P_l(\cos\theta_2) \tag{7}$$

where $U_l^{\pm}(k_p, r)$ satisfies

$$\left[\frac{\mathrm{d}^2}{\mathrm{d}r^2} + k_p^2 - \frac{l(l+1)}{r^2} - 2V_{1s,1s}(r) - 2V_{\mathrm{pol}}(r)\right] U_l^{\pm}(k_p r) = \pm \chi_l^{\pm}(r) r R_{1s}(r) \tag{8}$$

with

$$\chi_l(r) = -(\varepsilon_{1s} - k_p^2)\delta_{l_0} \int_0^{\infty} t R_{1s}(t) U_l(k_p t)\mathrm{d}t$$

$$-\frac{2}{2l+1}\int_0^{\infty} t R_{1s}(t) U_l(k_p t) r_l(t, r)\mathrm{d}t \tag{9}$$

and

$$r_l(t, r) = \frac{r_<^l}{r_>^{l+1}}.$$

The boundary conditions are

$$U_l(k_p, 0) = 0$$

$$U_l(k_p, r) \underset{r\to\infty}{\sim} k_p^{-1/2}\sin(\phi(r) + \delta_l)$$

with

$$\phi(r) \underset{r\to\infty}{\sim} kr - \frac{1}{2}l\pi + \frac{Z}{k}\ln 2kr + \eta_l$$

where

$$\eta_l(k) = \arg\Gamma\left(l + 1 - \frac{iZ}{k}\right).$$

The direct static potential $V_{1s,1s}(r_2)$ is given by

$$V_{1s,1s}(r_2) = \frac{-(Z-1)}{r_2} - \left(Z + \frac{1}{r_2}\right)\exp(-2Z)r_2, \tag{10}$$

and

$$V_{\text{pol}}(r_2) = \frac{-9}{4x^4}\left[1 - \exp(-2x)\left(1 + 2x + 2x^2 + \frac{4}{3}x^3 + \frac{2}{3}x^4 + \frac{4}{27}x^5\right)\right], \quad (11)$$

in which $x = Zr_2$.

Finally the differential cross-sections are obtained by using the formula

$$\frac{d\sigma}{d\Omega} = \frac{\mu^2}{4\pi^2}\frac{k_q}{k_p}|T_{pq}|^2 \quad (12)$$

where

$$|T_{pq}|^2 = \tfrac{1}{4}(|T_{pq}^+|^2 + 3|T_{pq}^-|^2). \quad (13)$$

In our approximation

$$T_{pq}^{\pm} = \left\langle \phi_q(\mathbf{r}_1)\chi_{kq}(Z,\mathbf{r}_2)\left|\frac{1}{r_{12}}\right|(1 + P_{12})\phi_p(\mathbf{r}_1)F^{\pm}(\mathbf{r}_2)\right\rangle \quad (14)$$

where P_{12} is the exchange operator.

Thus

$$T_{pq}^{\pm} = 2\pi(f^{\pm} \pm g^{\pm}) \quad (15)$$

where

$$f^{\pm}(\mathbf{k}_p, \mathbf{k}_q) = \frac{1}{2\pi}\int d\mathbf{r}_1 \int d\mathbf{r}_2 \phi_q^*(Z,\mathbf{r}_1)\frac{1}{r_{12}}\phi_p(Z,\mathbf{r}_1)F^{\pm}(\mathbf{r}_2)\chi_{kq}^*(Z,\mathbf{r}_2). \quad (16)$$

$$g^{\pm}(\mathbf{k}_p, \mathbf{k}_q) = \frac{1}{2\pi}\int d\mathbf{r}_1 \int d\mathbf{r}_2 \phi_q^*(Z,\mathbf{r}_1)\frac{1}{r_{12}}\phi_p(Z,\mathbf{r}_2)F^{\pm}(\mathbf{r}_1)\chi_{kq}^*(Z,\mathbf{r}_2). \quad (17)$$

All the symbols used have already been defined by McDowell *et al* (1973). $\chi_{kq}^*(Z,\mathbf{r}_2)$ is the outgoing Coulomb wave-function of an electron in the field of nucleus of charge Z.

In order to calculate the total and differential cross-sections we make the angular momentum expansion for $\chi_{kq}^*(Z,\mathbf{r}_2)$ and $F^{\pm}(\mathbf{r}_2)$ and write

$$T_{pq}^{\pm} = \sum_{l=0}^{\infty} B_l^{\pm} P_l(\cos\theta) \quad (18)$$

where

$$B_l^{\pm} = \frac{4\pi}{\sqrt{k_p}}\exp(i\zeta_l^{\pm})[(2l+1)I_A + I_B] \quad (19)$$

with

$$I_A = \int_0^{\infty} U_l^{\pm}(k_p, r_2)H_l(k_q, r_2)f_{1s,ns}(r_2)r_2\,dr_2 \quad (20)$$

$$I_B = \int_0^{\infty} R_{ns}(r_1)U_l^{\pm}(k_p, r_1)g_{1s,l}(r_1)dr_1 \quad (21)$$

and

$$H_l(k_q, r_2) = G_l(k_q, Z, r_2)/k_q r_2 \quad (22)$$

where $G_l(k_q, Z, r_2)$ is the regular lth order Coulomb function. $f_{1s,ns}(r_2)$ and $g_{1s,l}(r_1)$

are given by

$$f_{1s,ns}(r_2) = \int_0^\infty R_{1s}(r_1) R_{ns}(r_1) \frac{1}{r_>} r_1^2 \, dr_1 \tag{23}$$

$$g_{1s,l}(r_1) = r_1 \int_0^\infty R_{1s}(r_2) H_l(k_f r_2) \frac{r_<^l}{r_>^{l+1}} r_2 \, dr_2. \tag{24}$$

The radial equation for $U_l^{\pm}(kr)$ (McDowell *et al* 1973) has been solved by a non-iterative procedure. The normalization and phase shift have been obtained by matching with JWKB solution. The numerical integrations for I_A and I_B have been done accurately using Simpson's rule.

3. Results and discussion

The cross-sections obtained in the present work are compared with those reported earlier using other theories (distorted wave models, close coupling as well as first Born approximation) and with experiments. Different distorted wave models differ from one another in that the distortion is taken in either initial or in the final channel (sometimes in both). It is, therefore, desirable to see how the results based on them differ from each other. In particular it would be interesting to compare the present results with those obtained by McDowell *et al.*

The total cross-sections obtained presently are close to 1*s*–2*s*–2*p* close coupling results throughout the energy range investigated and also compare well with VCCPBA calculations (see figure 1). In comparison to DWPO I and VCCPBA results the present calculations show better agreement with experimental measurements at high energies. The present calculations agree well with experimental results also in the energy range 4·00–7·35 Ryd. Below 4 Ryd the present results are larger than the experimental ones whereas the DWPOI and the VCCPB results are in close agreement with the latter. The disagreement of DWPO I results with the present calculations is maximum below 4 Ryd and decreases with increase in incident energy. For energies greater than 7·35 Ryd, all the calculated curves fall into a relatively narrow band. In the case of 1*s*–2*s* excitation of hydrogen it is found that the Born approximation calculation is in good agreement with the experimental data at low energies and beyond 100 eV the disagreement of the calculated cross-sections under the various approximations with experimental results is not reduced with increase in energy. This seems to be a special feature of the 1*s*–2*s* excitation of hydrogen in contrast to other transitions in hydrogen, although the reason for this is not clear.

Our differential cross-sections at an incident electron energy of 7·35 Ryd for 1*s*–2*s* transition with other theoretical results have been presented in figure 2. The comparison of the present results with those from the DWPO III calculation shows that the inclusion of Coulomb wave (in place of plane waves) in the final channel has gradually lesser effect as the scattering angle increases. At large scattering angles our results are lower than the DWPO III results. The present cross-section results are larger for small scattering angles up to 25° but are smaller for the large angles as compared to the CPBA results. These features may be attributed to the fact that at large scattering angles polarization effectively reduces the effect of the full nuclear charge (see figure 1(d) of Stauffer and Morgan (1975)). Table 1 shows the cross-sections

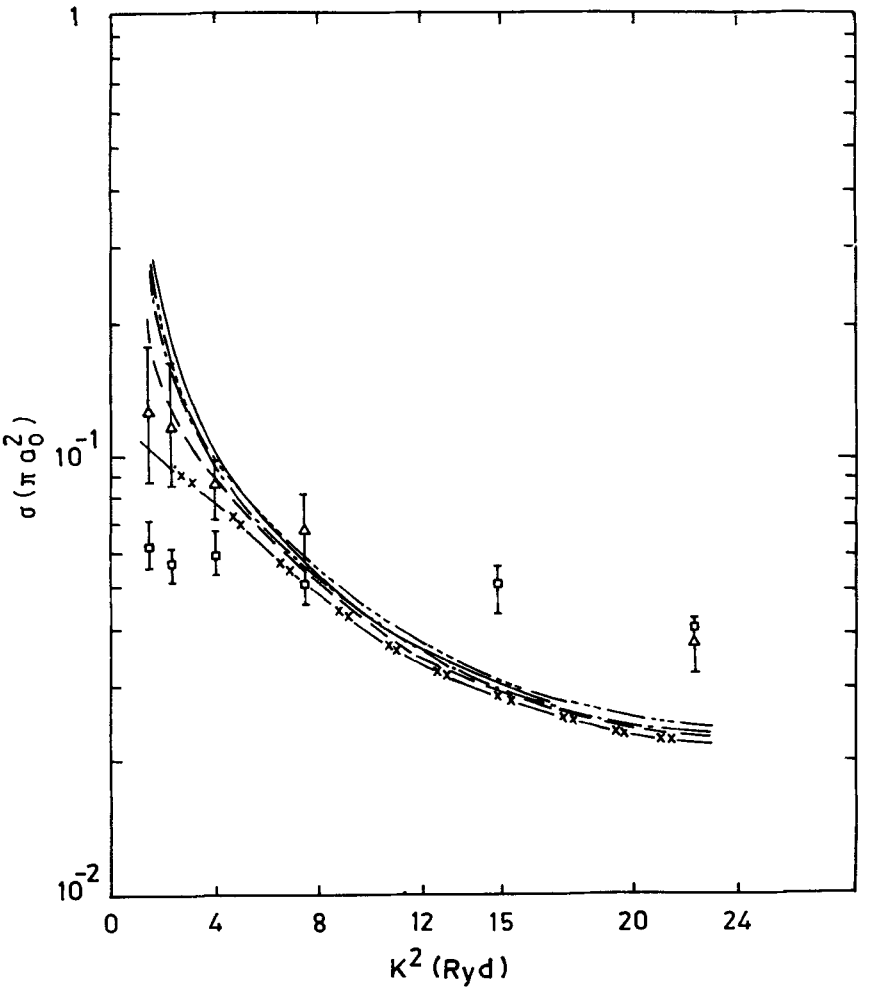

Figure 1. Total $1s$–$2s$ cross-sections $\sigma(\pi a_0^2)$ plotted against energy (Ryd) for electron scattering from H——— Present, – – –, VCCPB results of Shaver and Stauffer (1980); ——× ×——, PWPO I results of McDowell *et al* (1973); ————– – –————, $1s$–$2s$–$2p$ close coupling results of Kingston *et al* (1976); ——·——, Born; □, experiment (Hills *et al* 1966); △, experiment (Kauppila *et al* 1970).

calculated in the present work both when polarization effect is included and when not included. We find that for large angles of scattering the cross sections without polarization are larger than when the polarization potential is included.

Figure 3 compares our differential cross-sections at 4 Ryd for $1s$–$2s$ transition obtained in this work with other theoretical results and the experimental measurements due to Williams (1981). Again we find that the present results are larger than the VCCPB results up to the scattering angle of 35° while at larger angles the former tend towards the DWPO III results. The present values are even larger than the experimentally measured values up to 20° but for larger scattering angles these are systematically lower. This latter feature is common to VCCPB and DWPO III calculations.

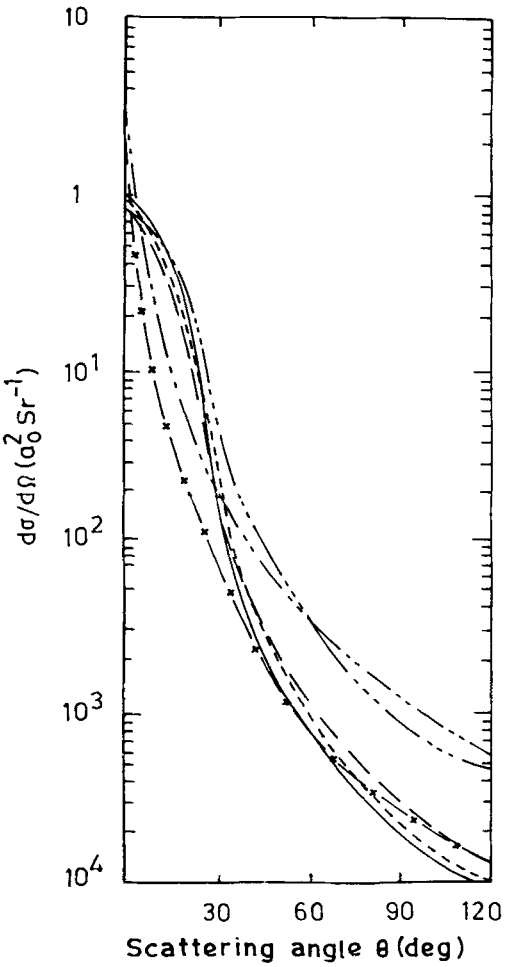

Figure 2. Differential cross-sections plotted against angle for 1*s*–2*s* transitions in $e^- + H$ scattering at 7·35 Ryd. ———, Present results; ———·——, 1*s*–2*s*–2*p* close coupling; ———···———, two-potential Born model used by Junker (1975); — — —, VCCPB; —— × ——, DWPO III model of Scott and McDowell (1977); -----, CPBA.

Our results for 1*s*–*ns* ($n = 2, 3$) transition are presented in table 1. We have compared the two sets of calculations with polarization potential (P) and without polarization potential (WP) to study the effect of polarization. The effect of inclusion of polarization potential to enhance the cross-sections diminishes gradually as the scattering angle increases because it reduces the effect of full nuclear charge at large scattering angles as pointed out earlier. The present result with polarization potential are compared with DWPO I calculation to see the effect of Coulomb waves. Inclusion of Coulomb waves in the final channel in the present calculations is seen to increase the cross-sections. The present results is almost identical to that reported by McDowell *et al* (1973) at an incident energy of 100 eV and scattering angle of 90° for the 1*s*–2*s* transition whereas the present value of the differential cross section obtained without the inclusion of the polarization potential is larger than that reported by McDowell

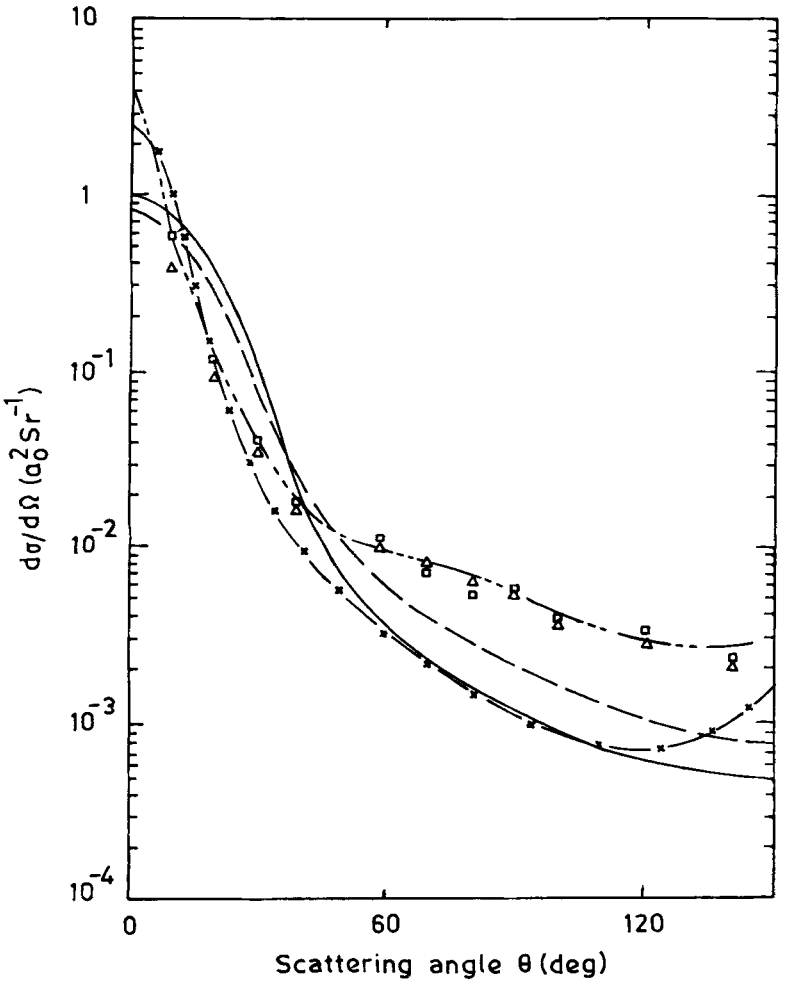

Figure 3. Differential cross-sections plotted against angle for $1s$–$2s$ transition in $e^- + H$ scattering of 4·0 Ryd. ———, Present; —— × —— DWPO III; ————·————, $1s$–$2s$–$2p$ close coupling; ———, VCCPB; □ and △, experiment (Williams 1981).

et al. The same is true in the case of $1s$–$3s$ transition. Despite the equality of the differential cross-sections at 90° the difference between the total cross-section obtained in the present work and that reported by McDowell *et al* at 100 eV for the $1s$–ns ($n = 2, 3$) transition is not unexpected since the major contribution to the total cross-section comes from the small scattering angle region.

Differential and total cross-sections for the $1s$–ns ($n = 2, 3, 4$) transition at various incident energies are compared with VCCPB results in table 2. Due to inclusion of polarization our results are higher than VCCPB results at scattering angles up to 120°, 90°, 90° and 45° at impact energies 1 Ryd, 1·21 Ryd, 1·44 Ryd and 2·25 Ryd respectively for $1s$–$2s$ transition. Our differential cross-sections are higher than VCCPB results up to 30° at 4 Ryd as well as 7·35 Ryd and up to 15° only at 14·70 Ryd impact energy in the case of $1s$–$3s$ and $1s$–$4s$ transitions. The total cross-sections are in agreement with VCCPB results in all cases.

Table 1. Differential cross-sections $d\sigma/d\Omega$ ($a_0^2 Sr^{-1}$) for $e + H(1s) \rightarrow e + H(ns)$.

E(Ryd)	Model	0	15	30	45	60	90	120	180	$\sigma(\pi a_0^2)$
1s–2s										
7·35	P	9·7, – 1	2·9, – 1	1·8, – 2	1·8, – 3	6·6, – 4	1·9, – 4	9·2, – 5	2·9, – 5	5·94, – 2
	WP	9·4, – 1	2·9, – 1	1·8, – 2	1·8, – 3	6·4, – 4	2·1, – 4	9·8, – 5	4·8, – 5	5·88, – 2
	McDowell	8·30, – 1			1·63, – 3		1·98, – 4			5·006, – 2
14·70	P	9·58, – 1	1·04, – 1	2·02, – 3	2·24, – 4	9·0, – 5	2·08, – 5	1·18, – 5	1·32, – 6	2·96, – 2
	WP	9·51, – 1	1·02, – 1	2·01, – 3	2·54, – 4	9·34, – 5	2·37, – 5	1·22, – 5	6·33, – 6	2·96, – 2
	McDowell	9·03, – 1			2·31, – 4		1·88, – 5			2·75, – 2
1s–3s										
7·35	P	1·43, – 1	6·00, – 2	5·43, – 3	5·15, – 4	1·64, – 4	4·66, – 5	2·08, – 5	1·29, – 5	1·17, – 2
	McDowell	1·12, – 1			4·39, – 4		4·61, – 5			9·70, – 3
14·70	P	1·41, – 1	2·64, – 2	6·07, – 4	6·27, – 5	2·22, – 5	5·74, – 6	2·48, – 6	1·14, – 6	5·90, – 3
	McDowell	1·24, – 1			5·61, – 5		5·15, – 6			5·398, – 3

P = Present; WP = Present neglecting polarization; McDowell = Reported by McDowell *et al* (1973).

Table 2. Differential cross-sections $d\sigma/d\Omega$ ($a_0^2 Sr^{-1}$) and total cross-section $\sigma(\pi a_0^2)$ for $1s \rightarrow ns$ ($n = 2, 3, 4$) excitation of hydrogen by electron impact.

E(Ryd)	Model	0°	15°	30°	45°	60°	90°	120°	180°	$\sigma(\pi a_0^2)$
1s–2s										
1·00	P	1·06, −00[+]	8·69, −1	4·75, −1	1·80, −1	6·55, −2	4·23, −2	2·98, −2	1·96, −2	4·45, −1
	VC	1·00, −1	8·66, −2	5·61, −2	2·80, −2	1·27, −2	1·28, −2	2·58, −2	4·01, −2	1·04, −1
1.21	P	1·04,00	8·22, −1	4·04, −1	1·37, −1	5·09, −2	2·80, −2	1·52, −2	1·00, −2	3·62, −1
	VC	2·21, −1	1·84, −1	1·07, −1	4·69, −2	1·92, −2	1·61, −2	2·88, −2	4·32, −2	1·50, −1
1·44	P	1·03,00	7·83, −1	3·47, −1	1·06, −1	3·92, −2	1·82, −2	8·73, −3	6·19, −3	3·04, −1
	VC	3·24, −1	2·58, −1	1·36, −1	5·39, −2	2·21, −2	1·61, −2	2·35, −2	3·31, −2	1·64, −2
2·25	P	1·01,00	6·75, −1	2·12, −1	4·78, −2	1·58, −2	5·40, −3	2·51, −3	1·72, −3	1·95, −1
	VC	5·25, −1	3·60, −1	1·33, −1	3·93, −2	1·65, −2	9·11, −3	7·64, −3	7·60, −3	1·36, −1
1s–3s										
4·0	P	1·46, −1	8·92, −2	2·14, −2	3·28, −3	9·34, −4	2·57, −4	1·24, −4	7·75, −5	2·17, −2
	VC	9·70, −2	6·30, −2	1·67, −2	3·49, −3	1·35, −3	5·16, −4	2·64, −4	1·50, −4	1·71, −2
7·35	P	1·43, −1	6·00, −2	5·43, −3	5·15, −4	1·64, −4	4·66, −5	2·08, −5	1·29, −5	1·17, −2
	VC	1·18, −1	5·06, −2	5·39, −3	7·66, −4	2·81, −4	7·14, −5	2·74, −5	1·38, −5	1·03, −2
14·70	P	1·41, −1	2·64, −2	6·07, −4	6·27, −5	2·22, −5	5·74, −6	2·48, −6	1·14, −6	5·90, −3
	VC	1·29, −1	2·47, −2	7·62, −4	1·05, −4	3·31, −5	6·64, −6	2·71, −6	1·46, −6	5·55, −3
1s–4s										
4·00	P	4·97, −2	3·17, −2	8·56, −3	1·39, −3	3·77, −4	1·03, −4	4·82, −5	3·77, −5	8·06, −3
	VC	3·21, −2	2·22, −2	6·50, −3	1·41, −3	5·39, −4	2·05, −4	1·06, −4	6·12, −5	6·30, −3
7·35	P	4·87, −2	2·21, −2	2·30, −3	2·08, −4	6·45, −5	1·77, −5	7·89, −6	3·95, −6	4·36, −3
	VC	3·79, −2	1·90, −2	2·19, −3	3·07, −4	1·10, −4	2·76, −5	1·10, −5	6·04, −6	3·82, −3
14·70	P	4·79, −2	1·04, −2	2·45, −4	2·48, −5	8·51, −6	2·31, −6	9·74, −7	7·11, −7	2·19, −3
	VC	4·36, −2	9·69, −3	3·07, −4	4·16, −5	1·26, −5	2·78, −6	1·01, −6	7·42, −7	2·06, −3

P = Present; VC = VCCPB; [+] Number following comma denotes the power of 10 by which the entry should be multiplied.

A critical analysis of our results reveals that as the impact energy increases the enhancement in cross-section due to inclusion of polarization becomes significant at relatively smaller angles. The experimental data presently available do not cover the low angle region well enough to allow a definite test of the importance of polarization at these angles. The calculations of the total cross-sections by the present method show good agreement with the available theoretical and experimental results over a wide range of energies. The difference between our calculations and other theoretical differential cross-sections at large scattering angles has no important role in the integrated cross-sections. In fact the main contribution to the total cross sections comes from scattering angles up to 30° where the present differential cross-sections are enhanced due to inclusion of both effects (polarization and Coulomb effects) leading to improvement in the total cross-sections.

Differential cross-sections for the $1s$–$2s$ and $1s$–$3s$ transitions in the case of He^+ at several impact energies are shown in figures 4 and 5. It is observed that the large angle contribution decreases considerably with increasing energy. Our results agree qualitatively with those of McDowell *et al* (1973).

Our results for $1s$–$2s$ transition of hydrogenic ions are presented in table 3 from threshold to $20Z^2$ Ryd. For $Z = 2, 6, 7$ our scaled cross-sections have been compared with DWPO II results of McDowell *et al* (1977) in table 4 for five values of E_z. It is

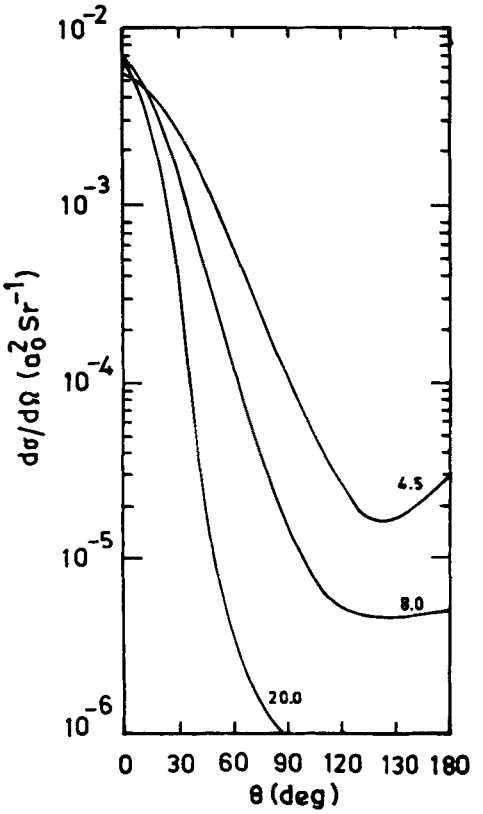

Figure 4. Differential cross-sections for the $1s$–$2s$ at various energies (k_i^2 Ryd) marked on the curves.

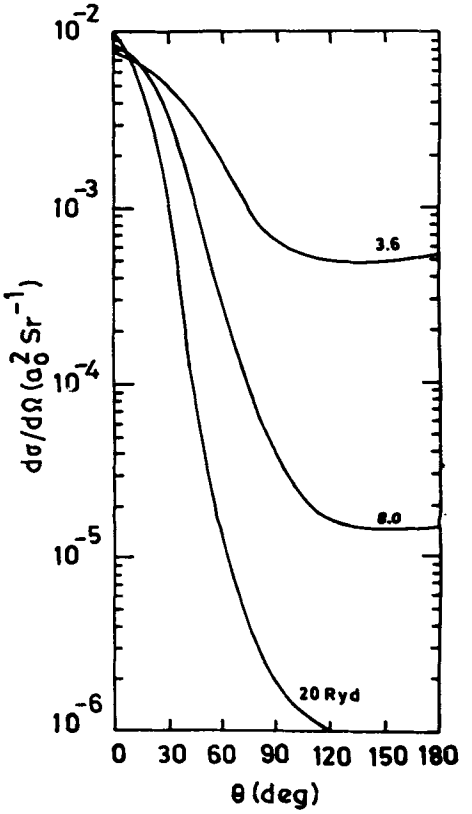

Figure 5. Caption same as in figure 4 for $1s$–$3s$ transition of He^+.

Table 3. Scaled cross-sections Z^4Q against scaled energy E_z for hydrogenic ions: $1s$–$2s$ (in units of πa_0^2).

E_z	1	2	6	7
0·7501	6·533, −1	5·924, −1	5·3076, −1	5·243, −1
0·7600	6·434, −1	5·853, −1	5·243, −1	5·180, −1
0·7800	6·175, −1	5·706, −1	5·117, −1	5·059, −1
0·8000	5·929, −1	5·570, −1	4·998, −1	4·941, −1
0·9000	5·033, −1	4·968, −1	4·467, −1	4·426, −1
1·000	4·441, −1	4·480, −1	4·055, −1	4·008, −1
2·000	2·194, −1	2·218, −1	2·068, −1	2·054, −1
4·000	1·092, −1	1·093, −1	1·048, −1	1·044, −1
6·000	7·260, −2	7·260, −2	7·057, −2	7·027, −2
8·000	5·437, −2	5·444, −2	5·323, −2	5·316, −2
10·000	4·336, −2	4·338, −2	4·269, −2	4·263, −2
15·000	2·840, −2	2·842, −2	2·814, −2	2·816, −2
20·000	2·069, −2	2·072, −2	2·056, −2	2·055, −2

observed that the present calculations are always higher than DWPO II results. For fixed E_z the ratio $(Q_{\text{present}}/Q_{\text{DWPO}})$ decreases with increasing Z. It seems that the difference between our approximation and that of McDowell *et al* (1977) becomes less important as the nuclear charge increases. We have used full nuclear charge Z

Table 4. Variation of Z^4Q with E_z for hydrogenic ions.

		$Z=2$			$Z=6$			$Z=7$		
	E_z	*a*	*b*	*a/b*	*a*	*b*	*a/b*	*a*	*b*	*a/b*
1*s*–2*s*	0·75	0·1592	0·1064	5·567	0·5307	0·3701	1·4339	0·5243	0·3883	1·3502
	1·0	0·4480	0·1538	2·9128	0·4055	0·3085	1·3144	0·4008	0·3182	1·2575
	2·0	0·2218	0·1406	1·577	0·2068	0·1791	1·154	0·2054	0·1816	1·1310
	4·0	0·1093	0·0877	1·246	0·1048	0·0978	1·070	0·1044	0·0984	1·060
	8·0	0·0544	0·0494	1·101	0·0532	0·0518	1·027	0·0531	0·0519	1·023

(a) present; (b) DWPO II of McDowell *et al* (1977)

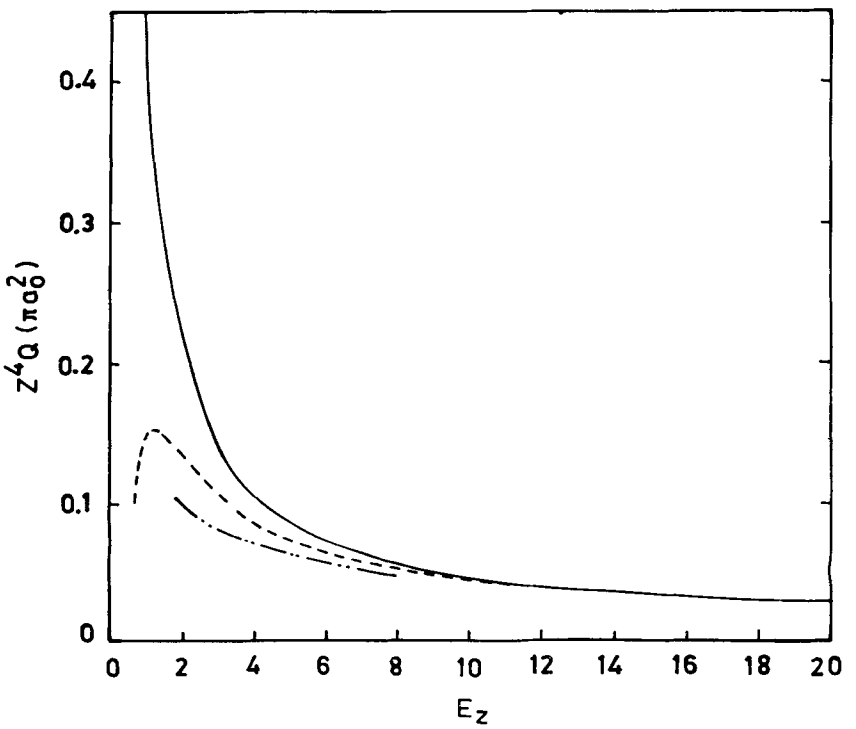

Figure 6. Excitation of He^+ (2*s*): ——— Present results, ---, DWPO II of McDowell *et al* (1977); ——··——, SOP (Bransden and Noble 1976).

whereas McDowell *et al* have taken $Z-1$ for the Coulomb waves in the final channel.

We compare our scaled total cross-sections with those of Bransden and Noble (1976) in the impact parameter second-order potential method (SOP) and DWPO II method of McDowell *et al* (1977) in figure 6 for 1*s*–2*s* excitation of He^+. The SOP results lie lowest and merge with the present calculations for $E_z > 8$, while the present values approach DWPO results from above and are in close agreement for $E_z > 9$. At high impact energies all the results are found to be identical.

From the above discussion we conclude that the present work provides an useful extension of the CPB method for electron-hydrogen collision at small scattering angles

above the twice threshold energy. In hydrogenic ions the present results are close to the DWPO I and II calculations of McDowell *et al* (1973 and 1977).

References

Bransden B H and Noble C 1976 *J. Phys.* **B9** 1507
Geltman S 1971 *J. Phys.* **B4** 1288
Geltman S and Hidalgo M B 1971 *J. Phys.* **B4** 1299
Hills D, Kleinpoppen H and Koschmieder H 1966 *Proc. Phys. Soc.* **89** 35
Junker B R 1975 *Phys. Rev.* **A11** 1552
Kauppila W E, Ott W R and Fite W L 1970 *Phys. Rev.* **A1** 1099
Kingston A E, Fon W C and Burke P G 1976 *J. Phys.* **B9** 605
McDowell M R C, Morgan L A and Myerscough V P 1973 *J. Phys.* **B6** 1435
McDowell M R C, Morgan L A, Myerscough V P and Scott T 1977 *J. Phys.* **B9** 2727
Schaub-Shaver J A and Stauffer A D 1980 *J. Phys.* **B13** 1457
Scott T and McDowell M R C 1977 *J. Phys.* **B10** 1059
Stauffer A D and Morgan L A 1975 *J. Phys.* **B8** 2172
Williams J F 1981 *J. Phys.* **B14** 1197